Arab J Sci Eng
DOI 10.1007/s13369-017-2478-2

RESEARCH ARTICLE - CHEMISTRY

Synthesis and Characterization of Tri-metallic Fe–Co–Ni Catalyst Supported on $CaCO_3$ for Multi-Walled Carbon Nanotubes Growth via Chemical Vapor Deposition Technique

A. S. Abdulkareem[1,3] · I. Kariim[1,3] · M. T. Bankole[2,3] · J. O. Tijani[2,3] · T. F. Abodunrin[3] · S. C. Olu[3]

Received: 23 August 2016 / Accepted: 6 March 2017

Abstract In this study, multi-walled carbon nanotubes (MWCNTs) were developed via the decomposition of acetylene gas over tri-metallic (Fe/Co/Ni) catalyst supported on $CaCO_3$ in a vapor deposition (CVD) reactor. The effects of mass of $CaCO_3$ support, pre-calcination temperature and pre-calcination time on the yield of catalyst were investigated and optimized using 2^3 factorial experimental design. The catalyst obtained at the optimal conditions was utilized for MWCNTs production using catalytic chemical vapor deposition method (CCVD). The effects of growing time and deposition temperatures on the yield of the MWCNTs were also studied. The as-synthesized catalyst and MWCNTs were characterized using the following analytical techniques: HRSEM, HRTEM, FTIR, TGA/DTA, EDS, XRD, and BET surface area. The results revealed that the optimal experimental conditions to obtain the maximum catalyst yield of 92.04% were: mass of $CaCO_3$ support of 8 g, pre-calcination temperature of 110 °C, and pre-calcination time of 8 h. The TGA and BET analysis showed that the catalyst developed at the optimal conditions were thermally stable with a high surface area of 224.68 m^2/g and particle size distribution in the ranges of 0.1–60 nm. The HRSEM and HRSEM micrograph revealed that the produced CNTs were multi-walled carbon nanotubes in nature comprises homogeneous well-aligned woven-like structure. XRD patterns confirmed that the produced MWCNTs were highly graphitized with little structural defects. This present work indicated that MWCNTs of uniform strands and controlled structure can be produced from tri-metallic (Fe/Co/Ni) catalyst supported on $CaCO_3$ through CCVD technique.

Keywords Tri-metallic catalyst · Wet impregnation · $CaCO_3$ · MWCNTs · Characterization · DLS-chat

1 Introduction

Since early 1991, the extensive and intensive synthesis of large quantities of well-defined array and high crystalline carbon nanotubes at a relatively low cost have attracted significant attention from governmental and non-governmental organization due to its remarkable and exceptional mechanical, electrical, chemical and thermal properties [1–6]. Carbon nanotubes stands as a hot and special advanced nanomaterial required for diverse technological applications owing to its small size, mesoporous nature, high chemical and thermal stabilities, and unique electrostatic interaction with pollutants compared to conventional activated carbon [2]. Despite the increasing applications of CNTs in field emission, drug delivery, sensors, solar cells, and thermal conductors, the low yield of CNTs produced via different techniques remains a serious setback hindering its availability for the aforementioned practical applications [3–5]. Hence, it is become imperative to develop cost-effective and sustainable method for CNTs production in large scale that will meet the consumers demand.

Different techniques such as laser ablation, arc discharge, plasma enhanced chemical vapor deposition, electrolysis, horizontal furnace, fluidized bed reactor, hydrothermal, sonochemical, alcohol catalytic chemical vapor deposition,

✉ J. O. Tijani
jimohtijani@futminna.edu.ng

1 Department of Chemical Engineering, Federal University of Technology Minna, P.M.B. 65, Minna, Niger State, Nigeria

2 Department of Chemistry, Federal University of Technology Minna, P.M.B. 65, Minna, Niger State, Nigeria

3 Nanotechnology Research Group, Center for Genetic Engineering and Biotechnology, Federal University of Technology Minna, P.M.B. 65, Minna, Niger State, Nigeria

Published online: 15 March 2017

and catalytic chemical vapor deposition have been utilized to produce carbon nanotubes [5,7,8]. However, the laser ablation and arc discharge are associated with low yield of CNTs, high cost of equipment and difficulty in scaling up [9,10]. Conversely, catalytic chemical vapor deposition (CCVD) appears most promising, simple, reproducible, and economical technique to obtain high-quality and well-aligned CNTs yield at significantly low temperature compared to other techniques [11]. The production of CNTs via CCVD technique is mostly accomplished using transition metals supported on different substrate in the presence of a carbon source. These transition metals can be used individually (monometallic) or in combined form (bimetallic, tri-metallic, or ternary catalyst) to produce different types of CNTs [1,12]. Nevertheless, the preparation of CNTs using tri-metallic catalysts is considered a facile route to obtain less agglomerated, homogeneous and high-quality CNTs with improved catalytic performance than single or bimetallic catalysts. Besides, tri-metallic catalysts also contributed to high CNTs yield, impaction of excellent mechanical strength, and catalytic activity on CNTs due to the existence of a synergetic effect between or among the concerns metals [4,6,10]. The quality and the yield including the CNTs growth rate depend largely on the appropriate carbon precursor, suitable synthesis parameters, and operating conditions [1,13]. For instance, straight hollow carbon materials can be readily obtained using linear hydrocarbons (methane and acetylene gas), while semi-curved CNTs can be produced by cyclic hydrocarbons (xylene, benzene, cyclohexane, and fullerene) [1]. Cheng et al. [13] synthesised MWCNTs using tri-metallic catalyst (Co–Fe–Ni) supported on nanocrystalline $CaCO_3$ in a CVD reactor using acetylene and nitrogen flow rate of 100 and 300 mL/min for 20 min reaction time at 800 °C. The authors reported maximum carbon yields of approximately 120% under the applied synthesis conditions. Allaedini et al. [1] prepared MWCNTs from an unsupported tri-metallic (Ni–Co–Fe) catalyst growth in a CVD reactor connected to methane gas used as a carbon source. The authors demonstrated that highly stable bamboo-shaped CNTs of BET surface area (36.8 m^2/g) could be readily prepared without support such as SiO_2, Al_2O_3, MgO, thus eliminate the challenges of purification often associated with the supported CNTs. It should however be mentioned that several attempts have been made to enhance CNTs preparation including structural properties determination and measurement as well as discovery new applications [14]. One of such approach considered necessary for the successful production of high-quality and high-quantity CNTs via the CCVD process is the selection of an appropriate catalyst support. For instance, porous materials such as zeolite are considered a superior substrate in the production of zeolite-supported catalysts [10]. However, studies have shown that porous material usually accumulate amorphous carbon in large quantity as evident during the catalytic decomposition of acetylene gas where the outer surface failed to produce CNTs and the inner centers were completely covered with amorphous carbon [13]. In order to overcome all these drawbacks associated with porous materials, in this study a non-porous, cheap and readily available substrate ($CaCO_3$) was selected as a support substrate in the production of MWCNTs by CCVD technique. $CaCO_3$ is known to suppress amorphous carbon formation and promote CNTs production. In addition, CaO obtained from the decomposition of $CaCO_3$ is environmental friendly and readily dissolved in dilute HNO_3 or HCl to obtain MWCNTs free of contaminants [9]. Studies have shown that combination of metallic particles such as Fe, Co, Ni, and Mo substantially improved the catalytic activity, life time, and CNTs yield more than individual metal due to lower melting point of the mixed catalysts [1,13].

Thus, to the best of our knowledge, no study has reported the synthesis and application of factorial design to optimize the production parameters on the yield of Fe–Co–Ni catalyst supported on $CaCO_3$ and quality of the multi-walled carbon nanotubes (MWCNTs). In this present study, we report the synthesis of tri-metallic catalyst (Fe–Ni–Co) supported on calcium carbonate using a wet impregnation method. The effects of mass of $CaCO_3$ support, pre-calcination temperature and pre-calcination time on the yield of catalyst using 2^3 factorial experimental designs were investigated. Subsequently, the catalyst obtained at the optimal conditions was further utilized for carbon nanotubes production using the CCVD method. The effects of time and temperatures on the yield of the MWCNTs were also studied. The degree of crystallinity (XRD), surface morphology and elemental analysis (HRSEM/EDX), surface functional group (FTIR), thermal stability (TGA), and surface area (BET) of the developed catalyst and MWCNTs were also examined.

2 Materials and Methods

2.1 Materials

Nickel nitrate hexahydrate $Ni(NO_3)_2 \cdot 6H_2O$, cobalt nitrate hexahydrate ($Co(NO_3)_2 \cdot 6H_2O$), Iron nitrate nonahydrate ($Fe(NO_3)_3 \cdot 9H_2O$), calcium trioxocarbonate ($CaCO_3$), and concentrated hydrochloric acid (H_2SO_4) supplied by Sigma-Aldrich were used without further purification. All reagents were of analytical grade with percentage purity of 95–99.99%. Acetylene and argon gases were supplied by British Oxygen Company/Brin's Oxygen Company (BOC Gases Plc, Lagos, Nigeria) with percentage purity of 99.99%.

2.2 Synthesis of Fe–Ni–Co/$CaCO_3$ Catalysts

In this study, the preparation of the supported catalyst was achieved using a wet impregnation method described as

Table 1 Experimental ranges and levels of the factors used in the factorial design for Fe–Co–Ni/$CaCO_3$ catalyst preparation

Variables	Mass of support (g)	Pre-calcination time (hours)	Pre-calcination temperature (°C)
Low level (−)	7.00	8	110
High level (+)	8.00	10	120

Table 2 2^3 Experimental design mix for Fe–Co–Ni/$CaCO_3$ catalyst preparation

Runs	Mass of support (g)	Pre-calcination temperature (°C)	Pre-calcination time (hours)	*A*	*B*	*C*
1	7	120	8	−	+	−
2	8	120	8	+	+	−
3	8	120	10	+	+	+
4	7	110	8	−	−	−
5	7	120	10	−	+	+
6	7	110	10	−	−	+
7	8	110	8	+	−	−
8	8	110	10	+	−	+

follows: The catalyst was prepared by weighing 4.04 g of $Fe(NO_3)_3 \cdot 9H_2O$, 2.91 g $Ni(NO_3)_2 \cdot 6H_2O$ and 2.91 g of $Co(NO_3)_2 \cdot 6H_2O$ and subsequently dissolved in 50 mL distilled water. Thereafter, $CaCO_3$ support (7 and 8 g) was measured separately and added to the mixture of Fe, Ni, and Co salts. The mixture was allowed to age for 60 min under constant stirring to ensure homogeneity of the mixture. The resulting slurry was partially dried at room temperature and later oven-dried separately at a temperature of 110 and 120 °C and pre-calcination time of 8 and 10 h in a furnace. The dried supported catalyst was cooled, grounded, and finally screened through a 150 µm sieve size. The fine powder (catalyst) obtained was then calcined at 500 °C for 12 h. The experimental ranges and levels of the parameters used in the factorial design for Fe–Co–Ni/$CaCO_3$ catalyst preparation are presented in Table 1

Table 2 depicts the experimental design mix for the development of Fe–Co–Ni/$CaCO_3$.

The catalysts yield was determined after calcination using the relationship presented in Eq. 1.

$$Y\,(\%) = \frac{W_A - W_B}{W_A} \times 100 \tag{1}$$

where Y represents the catalyst yield (%), W_A is the weight of sample before calcination in gram, and W_B is the weight of sample after calcination also in gram.

2.3 Production of CNTs

CNTs were synthesized using catalytic chemical vapor deposition techniques. 1.0 g of the synthesized $CaCO_3$ supported Fe–Co–Ni tri-metallic catalyst was weighed and spread evenly on ceramic boat placed at the center of a cylindrical quartz tube reactor of length 101 cm with internal and external diameter of 5.2 and 6.0 cm respectively. The argon gas was introduced into the reacting furnace at initial flow rate of 30 mL/min to heat-up the catalyst and heating rate was controlled at 10 °C/min until the desired temperature was reached. The carrier gas (argon) flow rate was raised to 350 mL/min, and the carbon source (acetylene gas) was introduced at flow rate of 100 mL/min to produce CNTs under the continuous flow of argon gas. The flow ratio of the two gases argon to acetylene used throughout the production process was 3.5:1. The deposition of carbon (CNTs growth) over 1 g catalyst (Fe–Co–Ni/$CaCO_3$) was monitored at different growth temperatures: 550, 600, 650,700, 750 and 800 °C) for different reaction time of 30, 40, 50, 60 and 70 min respectively. The reaction was allowed to proceed until the specified reaction time was attained after which the acetylene flow was stopped and argon flow was continuously filled into a reaction chamber till the furnace cooled to room temperature. The ceramic boat was then removed from the quartz tube and weighed to determine the CNTs yield using Eq. (2).

$$\text{Yield}\,(\%) = \left(\frac{W_2 - W_1}{W_1}\right) \times 100 \tag{2}$$

where W_1 is the initial weight of the catalyst before reaction and W_2 is the weight of catalyst and carbon deposited after synthesis. The rate of carbon nanotubes deposition was evaluated using Eq. (3).

$$R(\%/\,\text{min}) = \left(\frac{y\,(\%)}{t\,(\text{min})}\right) \tag{3}$$

where R is the rate of carbon deposition (%/min), y is the carbon yield (%) and t is the residence time of the reaction (min) [15,16].

2.4 Factorial Design of Experiment

The development of an ideal catalyst for carbon nanotubes production (CNTs) can be achieved through optimization of the synthesis parameters that influence the growth process. The review of literature revealed that limited information exist on the optimization of effects of preparation parameters on the quantity and quality of catalysts and CNTs. The optimization of one variable at a time and keeping others constant may not guarantee establishment of optimum condition. This often led to time wastage due to large number of

experiment required. Thus, to produce near to ideal carbon nanostructures, factorial design is considered among other designs under response surface method (RSM) as a viable tool in the optimization of the reaction parameters to achieve better response. As a matter of fact, designed of experiment can be applied to reduce the number of experiment and the effects and the interactions of the main parameters based on the response can be easily estimated. Different parameters such as the effects of mass of $CaCO_3$ support, pre-calcination temperature and pre-calcination time on the yield of catalyst were considered as input variables in the factorial design. Typically, a two-level factorial design containing three factors was used as shown in Table 1. The level of the parameters varied for the optimization were selected following preliminary studies by [11] and were taken as the operating limit referred to as lower and upper levels. The lower levels (−) indicate variable values that were considered as lower limits and the high level (+) depict the variable values considered as upper limits. Center composite design is characterized by three operations namely; 2n axial runs, 2*n* factorial runs, and six center runs. In this case, n represent number of variables which is equal to 3 and the factorial design is translated into 8 runs. The statistical analysis was done using licensed Minitab ANOVA, and response optimization was conducted using factorial design and single catalyst with the best yield from optimization of three catalyst synthesis parameters for carbon nanotubes production. In the production of CNTs, effects of two variables such as growing time and deposition temperatures and their interactions on the yield of CNTs were also estimated

2.5 Characterization of the Synthesized Fe–Co–Ni/$CaCO_3$ and CNTs

The mineralogical composition of as-synthesised catalyst and MWCNTs were identified using powder X-ray diffraction analysis, performed on a Bruker AXS D8 Advance with Cu-Kα radiation with the acceleration voltage 40 kV, and scan velocity current 40 mA. The morphologies of the synthesised materials were examined using Zeiss Auriga HRSEM under the following operation conditions: current 10 mA, voltage 5 kV, aperture 0.4 mm and working distance 4–10.4 mm. A mass of 0.05 mg prepared samples were sprinkled on carbon adhesive tape and sputter coated with Au-Pd using Quorum T15OT for 5 min prior to analysis. The microscope was operated with electron high tension (EHT) of 5 kV for imaging. HRSEM equipped with EDS was further used to determine the elemental composition of the synthesised catalysts. The microstructure determination of the prepared catalysts and MWCNTs was done using a Zeiss Auriga high-resolution transmission electron microscope (HRTEM). Approximately, 0.02 g of the synthesised products was suspended in 10 mL methanol and thereafter subjected to ultra-sonication until complete dispersion was achieved. One or two drops of the slurry was dropped onto a holey carbon grid with the aid of a micropipette and subsequently dried via exposure to photo light prior to imaging. Thermal profiles of $CaCO_3$ support, the catalysts and MWCNTs were performed by Perkin Elma STA 4000. A 25-mg sample was placed in a sample pan, and the thermal behavior of the materials was investigated from 50° to 800 °C with a heating rate of 10 °C/min. Over these temperature range, nitrogen operating at a flow rate of 20 mL/min was used as purging gas. PerkinElmer 100 FTIR Spectrometer model "Spectrum Two" was used to identify the possible functional groups in the synthesised materials using the following instrumental settings: Force gauge: 50, scan wavelength: 4000–400 cm^{-1}, scan number: 4, unit: %Transmittance was used for the analysis. The FTIR probe was first cleaned with ethanol and the baseline was run to guard against interference. Taking into cognisance the aforementioned instrumental conditions, a 0.005 g sample was placed directly under the probe. This was followed by scanning and spectra corresponding to each individual sample were collected after the peaks were smoothened. For BET N_2 adsorption, about 100 mg of the dry powder sample in a sample tube was first degassed at 90 °C for 4 h to remove residual water and other volatile components that were likely to block the pores. The BET surface area and average pore volume distributions were obtained from the plot of volume adsorbed (cm^3/g STP) versus relative pressure. The N_2 adsorption–desorption isotherms were collected at −196 °C using Micromeritics ASAP 2020 Accelerated Surface Area and Porosimetry analyzer.

3 Results and Discussion

3.1 TGA and BET Analysis of $CaCO_3$

A supported metallic catalyst with a large surface area and maximum specific activity is a prerequisite for large scale production of quality CNTs via a CCVD method. In view of the significance of support on the stability of metallic catalyst, the support material ($CaCO_3$) was characterized to determine its stability and suitability for CNTs production. Studies have shown that high-quality catalyst can be produced by the deposition of an active metal component on a surface and pores of support material [7,8]. For proper dispersion of active metal on a support, the support must be highly porous, thermally stable with high surface area and excellent mechanical strength. Based on this reason, the thermal stability of $CaCO_3$ in N_2 atmosphere was investigated and the result obtained in the temperature range of 50–850 °C is shown in Fig. 1.

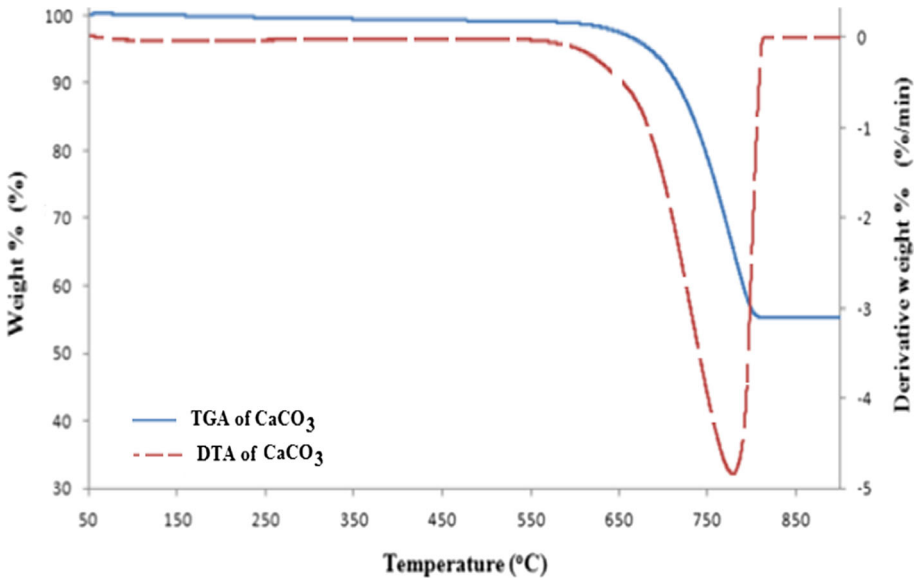

Fig. 1 TGA/DTA of calcium carbonate support in nitrogen environment

Table 3 Comparison of TGA result with the stoichiometry results of individual component in calcium carbonate sample

Material	Weight from TGA (mg)	Weight from Stoichiometry (mg)
$CaCO_3$	99.00	100.10
CO_2	42.00	43.97
CaO	57.01	55.98

According to Fig. 1, the support substrate ($CaCO_3$) was stable from 50 to 650 °C with no weight loss and afterward the $CaCO_3$ started to decompose forming CaO and probably CO/CO_2 respectively. It should be noted that only one degradation step from 650 to 820 °C was observed, which shows that, the support substrate was stable up till 650 °C. However, after 820 °C about 40% weight loss was observed when compared to the original or perhaps initial mass as shown in Table 3.

This mass loss was linked to the evolution of CO_2 and formation of residual CaO. The CO_2 evolved during the decomposition of $CaCO_3$ as shown in Eq. (4) has been reported to prevent catalyst poisoning and also reduce the polymerization of acetylene during the CNTs production [17]. The TGA result is closely related with the stoichiometry of calcium carbonate decomposition reaction owing to high level of accuracy for dependency. Meanwhile, the peak temperature as determined from the DTA curve of 771 °C represents the peak degradation temperature (T_p). It can be seen from Fig. 1 that $CaCO_3$ utilized as support in this study is thermally stable and can withstand calcination temperature of 500 °C adopted in this study.

$$CaCO_{3(s)} \longrightarrow CaO_{(s)} + CO_{2(g)} \quad (4)$$

Table 4 Results of 2^3experimental designs for Fe–Co–Ni/$CaCO_3$ catalyst preparation

Runs	mass of support (g)	Pre-calcination temperature (°C)	Pre-calcination time (h)	Catalyst yield (%)
1	7	120	8	90.54
2	8	120	8	91.58
3	8	120	10	86.02
4	7	110	8	87.96
5	7	120	10	89.76
6	7	110	10	89.94
7	8	110	8	92.04
8	8	110	10	85.70

Furthermore, the BET specific surface area of $CaCO_3$ was determined to be 3.8 m^2/g. This result agrees with the value reported by Mhlanga et al. [17] which shows that the support material has the required surface area to host the metallic particles.

3.2 Characterization of Fe–Co–Ni/$CaCO_3$

The influence of synthesis parameters such as: mass of support, pre-calcination temperature and pre-calcination time on the catalyst yield using 2^3 factorial experimental designs were investigated. Each of the factors was considered at lower and upper level and the results obtained are presented in Table 4.

According to Table 4, when the mass of support was 7 g at constant pre-calcination temperature 120 °C and pre-calcination time of 8 h, the catalyst yield was 90.54% (Runs 1). With an increase in the mass of support to 8 g under the same conditions as 7 g, the catalyst yield was 91.58% (Runs 2). From runs 3 to run 6, the catalyst yield was lower than the

Table 5 Summary of the observed peaks

Wavelength (cm^{-1})	Assigned group
3648	Water of crystallization
712 and 1414	NO_2 bending and stretching mode
1798	O=C=O bending mode

obtainable value at runs 1 and 2 irrespective of mass of support, pre-calcination temperature and pre-calcination time. Conversely, at experimental run 7 under similar conditions with runs 2 except pre-calcination temperature (110 °C), the catalyst yield was 92.04%. Furthermore, when the mass of support was 8 g, similar to runs 6, the obtained catalyst yield was 85.70%. Critical analysis of the results shows that the highest catalyst yield was 92.04% under the optimal conditions of mass of support (8 g), pre-calcination (110 °C) and pre-calcination time (8 h). Furthermore, it can be seen that even though combination of factors possibly influenced the yield, mass of support played major role on the catalyst yield than other parameters. Very importantly, there is a direct relationship between the mass of the support and catalyst yield. An increase in the mass of support from 7 to 8 g at constant pre-calcination temperature of 120 °C and drying time 8 h resulted to increase in the catalyst yield from 90.45 to 91.58%. The increased catalyst yield owing to increment in mass of support can be attributed to the availability of more pore spaces/opening in the support, which enable easy dispersion and penetration of the catalyst particles during the wet impregnation process. The catalysts obtained at optimal conditions (mass of support (8 g), pre-calcination (110 °C), and pre-calcination time (8 h) were then characterized, and the results obtained are presented as follows.

3.3 TGA Profile of Fe–Co–Ni Supported on $CaCO_3$

The thermal response of the tri-metallic catalyst (Fe–Co–Ni) supported on $CaCO_3$ heated under N_2 atmosphere was investigated using Thermogravimetric analysis (TGA) and the results obtained are displayed in Fig. 2.

Figure 2 illustrates the weight loss versus the applied temperature and was done to obtain information on the suitability of the catalyst for CNTs growth in a CVD reactor operated using a minimum and maximum temperature of 550 to 855 °C. As shown in Fig. 2, a mono-degraded temperature pattern without any significant weight loss before 600 °C was observed. This means that the catalyst support was stable up to 600 °C. This thermal profile agreed with the previous literature reports. For instance, Chiwaye et al. [10] found that $CaCO_3$ was stable up to 600 °C and later decompose at 610–810 °C to CaO and CO_2. On the other hand, Schmitt et al. [18] stated that complete decomposition of $CaCO_3$ to

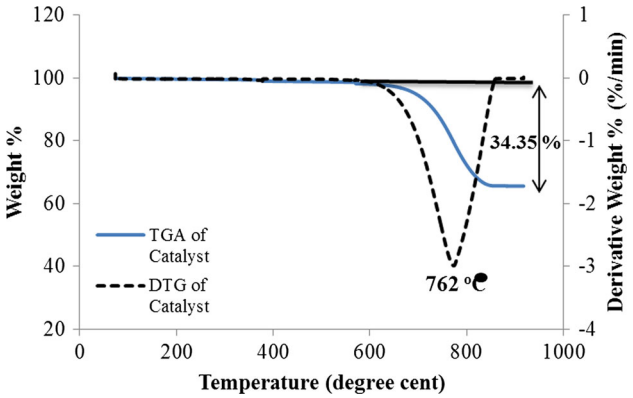

Fig. 2 TGA/DTA of tri-metallic Catalyst (Fe–Co–Ni/$CaCO_3$) under N_2 environment

CaO and CO_2 occurred at 700 °C. The differences in the stability of $CaCO_3$ may be linked to discrepancies in the heating rate and mass of $CaCO_3$. More so, the weight loss of <34.35% noticed over the temperatures range of 600–855 °C was attributed to $CaCO_3$ decomposition leading to formation of CaO and evolution of CO/CO_2, respectively. The mass loss may also be linked to the conversion of the loaded metal salts to their respective combined metal oxides such as $CoFe_2O_4$, $NiFe_2O_4$ and $NiCoFe_2O_4$, The evolution of CO_2 which occurred when Fe, Co and Ni salts reacted with $CaCO_3$ forming various combined metallic oxides may possibly be responsible for the observed mass loss. The formation of these metallic oxides corroborated the XRD pattern shown in Fig. 3.

3.4 BET Surface Area Analysis of Fe–Co–Ni Supported on $CaCO_3$

The specific surface area of the synthesised catalyst was measured using the BET nitrogen adsorption. The results obtained reveals that the surface area of 224.68 m^2/g for the synthesised catalyst. It was noticed that the surface area of the prepared tri-metallic catalyst improved significantly relative to the starting material $CaCO_3$ which is 3.8 m^2/g. The possible increase in surface area may be due to the loss of CO_2 during the impregnation stage and conversion of the metal salts into their respective combined oxides. This phenomenon created more openings on the support for easy penetration of metallic particles into the pores of the catalyst support. The micropore volume and the pore size of the synthesised catalyst were determined to be 0.081 cm^3/g and 3.017 nm respectively. This property of pore volume and pore size as determined under liquid nitrogen environment is an indication of the catalyst activeness and efficiency for its suitability of MWCNTs synthesis in a CVD reactor.

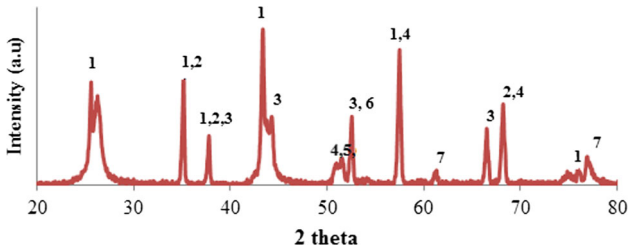

Fig. 3 XRD spectra of Fe–Co–Ni/ $CaCO_3$ catalyst (*1* $CaCO_3$, *2* $Ca_2Fe_2O_5/Fe_2O_3$, *3* CoO, *4* $CoFe_2O_4$, *5* $NiFe_2O_4$, *6* $Ca_2Fe_2O_5$, *7* CaO)

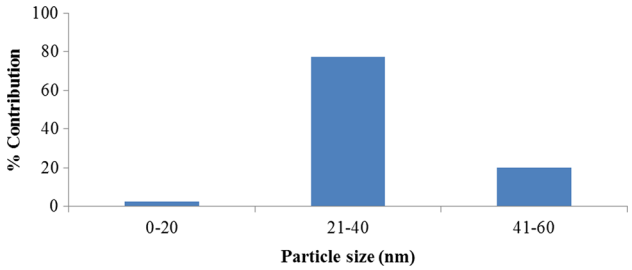

Fig. 4 Crystalline size distribution of Fe–Co–Ni/$CaCO_3$ catalyst

3.5 XRD Pattern of Fe–Co–Ni Supported on $CaCO_3$

Figure 3 displays the XRD pattern of the tri-metallic Fe–Co–Ni catalyst supported on $CaCO_3$.

The diffractions peaks observed at 2 theta values of 26°, 33°, 37°, 43°, 52°, 54°, 57°, 61°, 66°, 68° and 77° corresponds to the following reflection crystal planes: (110), (111), (111), (200), (211), (000), (220), (000), (111) and (222), respectively. The XRD pattern observed corresponds to different phases. For instance, the diffraction peaks observed at 2 theta value of 26° and 33° was assigned to $CaCO_3$ and mixture of $Ca_2Fe_2O_5/Fe_2O_3$. The formation of these mixed oxides has been previously reported [11]. For instance, Baghat et al. [9] observed the formation $Ca_2Fe_2O_5$ at 2 theta value of 33.2° for MWCNTs obtained from bimetallic Fe − $Co/CaCO_3$ catalyst but failed to explain the chemistry behind its formation. In contrast, Chiwaye et al. [10] attributed the formation of $Ca_2Fe_2O_5$ between 450 and 500 °C to the reaction between iron nitrate salt and the support material ($CaCO_3$). The characteristic peaks at 2θ of 37°, 43°, 57°, and 68° were assigned to Fe_2O_3, CoO and $CoFe_2O_4$, respectively. These metallic oxides were formed due to reaction between $Fe(NO_3)_3 \cdot 9H_2O$ and $Co(NO_3)_2 \cdot 6H_2O$. Moreso, the 2θ equals 52° and 54° represents possible reflection peaks of $NiFe_2O_3$ and $Ca_2Fe_2O_5$ which were formed due to the reaction between $Fe(NO_3)_3 \cdot 9H_2O$, $Ni(NO_3)_2 \cdot 6H_2O$ and $CaCO_3$ [9]. The formation of cobalt ferrite ($CoFe_2O_4$) agrees with the findings of Magrez et al. [19] and Li et al. [20] who independently in their study observed the formation of $CoFe_2O_4$ when Fe–Co catalyst supported on $CaCO_3$ was heated at 700 °C. Meanwhile, the reflection at 2θ equals 66° indicates the possible presence of a complex metallic oxide $NiCoFe_2O_3$. While the diffraction peaks observed at 61°, 66° and 77° were assigned to CaO and mixture of $CaCO_3$/CaO and CaO was formed due to decomposition of $CaCO_3$.

Critical analysis of the XRD pattern reveals the presence of $CaCO_3$ peaks, combined or mixed metal oxides, and complex metallic oxides, thus confirming the dispersion and reaction between the individual metal catalyst particles and the $CaCO_3$. However, the absence or non-detection of the individual elements (Fe, Co or Ni) by XRD, suggested that the small size nature, high dispersion or perhaps low concentration of the metallic particles in the catalyst mixture. The crystalline particles size (nm) of the tri-metallic catalyst developed was determined using the Scherrer equation shown in Eq. (5).

$$D = \frac{K\lambda}{\beta \cos\theta} \tag{5}$$

where D is the particle size diameter, β is the full width at half maximum, θ is the diffraction angle, λ is wave length of X-ray (0.1541 nm) and K is Scherrer constant (0.94). The crystalline particle size distribution of the developed catalyst is shown in Fig. 4.

The result indicates that the particle size of the synthesised catalyst is in the ranges of 0.1–60 nm while the average size was 29.02 nm.

3.6 HRSEM Analysis of Fe–Co–Ni/$CaCO_3$

The surface morphology of the developed catalyst was examined using high-resolution scanning electron microscope at low and high magnification as shown in Fig. 5.

The HRSEM micrographs revealed that the presence of a homogeneously distributed dense and agglomerated plate-like metallic particles on the surface of the support substrate. The micrograph also reveals that the synthesised catalyst was porous and thus would aid the diffusion of the carbon source to the active site of the catalyst during CNTs growth.

The elemental composition of the prepared catalyst was investigated using energy-dispersive X-ray spectroscopy. The EDS was recorded in the binding energy region of 0–12.5 KeV as shown in Fig. 6.

The EDS spectral revealed the presence of Fe, Co, Ni, Ca, O, C in different proportion. The atomic percentage of Fe, Co, Ni, Ca, O and C are 2.16, 2.17, 1.84, 18.19, 42.72 and 32.9% respectively. The peaks of Fe, Co, and Ni were insignificant compared to Ca, O and C which can be ascribed to their content in the catalyst mixture. Furthermore, it can be noticed from Fig. 6 that oxygen has the highest atomic percentage content of 32.9%. This could be attributed to the formation of metallic oxides in the catalyst mixture during

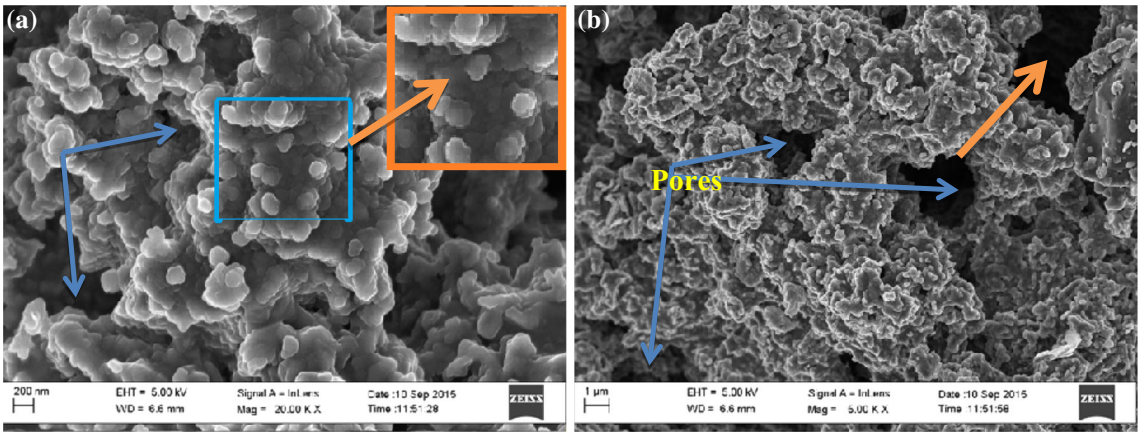

Fig. 5 HRSEM of Fe–Co–Ni/ $CaCO_3$ catalyst at **a** high and **b** low magnification

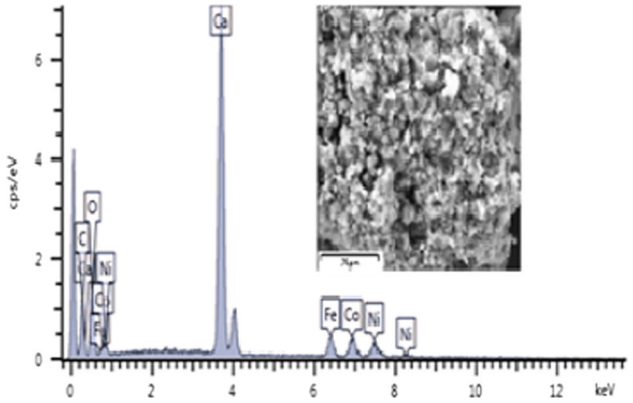

Fig. 6 EDS of tri-metallic catalyst (Fe–Co–Ni) on $CaCO_3$

the calcination process. Also, Fe, Co and Ni were observed at two different energy levels: low and high energy levels. This behavior shows that their respective oxides were present in the catalyst sample. Therefore, the presence of calcium carbonate combined complex metallic oxides and calcium oxide corroborated the XRD and TGA results shown in Figs. 2 and 3 respectively.

3.7 Effect of Reaction Time on the Synthesis of Carbon Nanotubes

The prepared catalysts at optimal conditions of mass of $CaCO_3$ support (8 g), pre-calcination (110 °C) and pre-calcination time (8 h) were further utilized to produce carbon nanotubes in catalytic vapor deposition reactor. Thereafter, the influence of reaction time and deposition on the morphologies, microstructures and the yields of the carbon nanotubes were investigated and the results obtained are presented in Fig. 7.

This experiment was done at constant temperature of 800 °C, argon flow rate of 100 mL/min and acetylene flow rate of 350 mL/min. It can be seen from the HRSEM micrographs (Fig. 7) that there is a variation in the morphology of the CNTs produced at different reaction time. At 30-min deposition time, the production of smaller-diameter CNTs was favoured due to low decomposition rate of acetylene gas occasioned with few active catalytic sites. Also, HRSEM micrographs in Fig. 7A consist of spongy-like thick CNTs encapsulated with amorphous carbon, metallic particles, and the residual CaO. Thus, the formation of low-quality MWCNTs (Fig. 7A) and low yield (Fig. 8) may be ascribed to low decomposition of acetylene gas on the catalyst nanoparticles. However, at 40-min interaction time, less fibrous and uniformly distributed CNTs of a sponge-like morphology were obtained (Fig. 7B). It was noticed that the level of aggregation specifically amount of metallic particles and possibly residual CaO reduced as the growing time was increased to 40 min. It is important to note that there were no clear differences in the CNTs structure produced at 50 and 60 min (Fig. 7C, D), an evidence of well-organized arrays of CNTs with less fibrous having a woven-like structure on the surface of the $CaCO_3$ supported tri-metallic catalyst was observed. This shows that increase in reaction time to 60 min did not influence the CNTs morphology. The possible reason proposed in this study for the formation of high-quality MWCNTs at 50 and 60 min may be attributed to the existence of equilibrium between the acetylene gas (carbon source) and the surface active sites of the prepared catalyst particles, such equilibrium contributed to the total decomposition of the acetylene in the CVD reactor.

With increase in the deposition time (60–70 min), short, thick and fibrous MWCNTs were observed. It is also evident from Fig. 7C, D, there is no much disparity in the HRSEM micrographs at 60 min and 70 min reaction time shown in Fig. 7D, E, aside from a slight destruction of the carbon nanostructures tubular morphology. It was noticed that as the reaction time increases, uniformly distributed thick and

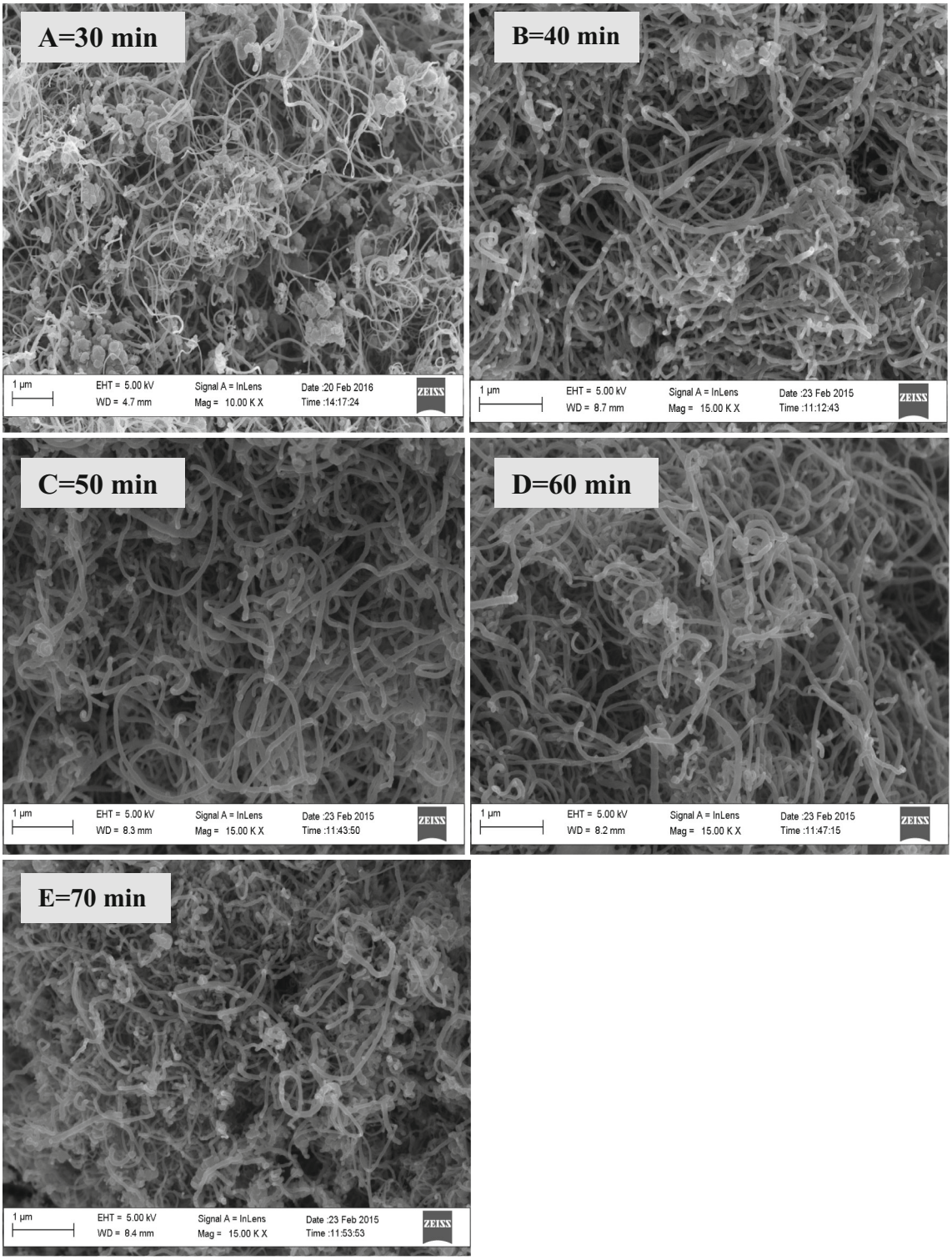

Fig. 7 HRSEM micrographs of CNTS produced at different reaction time

fibrous carbon deposits transformed into a loosely tiny bound tubular-like structure. It found that the diameter of the prepared CNTs look similar which is in accordance with the work of Khavarian et al. [21]. The authors found that average diameter of CNTs were not affected by the increase in the synthesis time and the reaction time. Contrary to Khavarian et al. [21], this study showed that well-organized arrays CNTs with little remnant of metallic particles and support

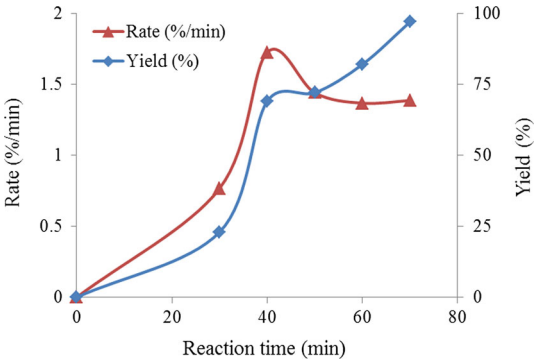

Fig. 8 Correlation chart of rate with yield and reaction time for MWCNTs yield

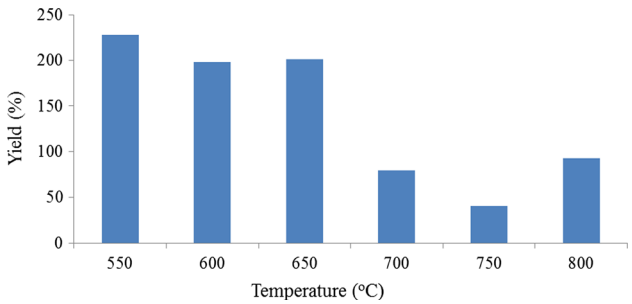

Fig. 9 Effect of reaction temperature on the percentage yield of MWCNTs at constant growing time of 70 min

material can be prepared at lower reaction time than at longer synthesis time.

Furthermore, the relationship between the yields of the carbon nanotubes as a function of reaction time was determined and presented in Fig. 8.

It can be observed (Fig. 8) that there is a direct linear relationship between the synthesis time and CNT yield, which means that an increase in the reaction time corresponds to increase CNTs yield. It was also observed that the production rate of MWCNTs increases from 0 to 1.75% as reaction time increases from 0 to 40 min and thereafter decreased with further increase in reaction time. The possible reason for the observed trend may be due to the presence of active pores and formability of dissociable carbide formation during the nucleation process of CNTs growth. The increase in the yields and quality of the CNTs as the growing time increases suggests that the catalysts were more active within this time range (0–40 min), thus responsible for better growth of CNTs. On the other hand, after 40 min, the production rate reduces indicating deactivation and decreased in the catalyst active site. In summary, shorter reaction times favoured the production of high-quality CNTs of higher aspect ratios than longer interaction times. Similar trend was reported by Kariim et al. [22] where the yield of the CNTs produced from $Fe-Ni/Al_2O_3$ catalyst reduced as the reaction time increased beyond 45 min. This observed trend in this study contradict the findings of Allaedini et al. [23] who reported that the decomposition rate of methane onto the catalyst particles reduces as the growing time increases due to cake formation on the CNTs layer which decreases the accessibility and catalysts activity.

3.8 Effect of Temperature on the CNTs Yield

The influence of production temperature on the microstructures, morphologies, and the yields of carbon nanotubes was also investigated. Studies have shown that temperature increment affects the geometry, diameter, and length of carbon nanotubes during the nucleation and growth process [24]. The results between acetylene decomposition (the yield of CNTs) at different applied temperatures are presented in Fig. 9.

According to Fig. 9, it was noticed that increase in the decomposition temperature from 550–800 °C corresponds to the decrease in CNTs yield. For instance, at operating temperature of 555 °C, the CNTs yield obtained was greater than 200%, and in contrast at 600 °C the CNT yield reduced to 200%. There was not much difference in the amount of carbon deposited at 600 and 650 °C. However, the amount of CNTs produced at 550 °C might not actually represent the truly deposited CNTs as other constituents such as $CaCO_3$ support and metallic particles might also add up to the yields owing to the stable nature of the two materials at this temperature as shown in Figs. 1 and 2. The decrease in CNT yields with increase in growing temperature observed in this study is however contradicting the trends reported by [23]. The authors demonstrated that the yield of CNTs produced at deposition temperature 550 °C was small compared to the amount of carbon material deposited at 750 °C. Whereas, in this study high yield of CNTs was observed at 550 °C. The discrepancies in the results obtained by this author as compared to this work may be due to difference in experimental conditions. In this study, the acetylene gas flow rate used was 100 mL/min compared to 1.5 mL/min flow rate of acetone used as a carbon precursor. This means that the rate of decomposition and deposition of acetylene gas used in this study was approximately 67 times greater than the rate utilized by [24]. This might possibly be responsible for the observed high yield of CNTs at 550 °C, which can be concluded that the activity of Fe–Co–Ni catalyst supported on $CaCO_3$ is high at this temperature.

On the other hand, when the decomposition temperature was raised to 750 °C, the CNTs yield decreased to <50%. The observed reduction in the CNTs yield is as a result of the equilibrium disturbance between the decomposition rate of acetylene gas and that of the diffusion rate of as-prepared carbon materials onto Fe–Co–Ni/$CaCO_3$ particles. Other observable influence of temperature on the yield of CNTs could possibly be linked to the formation of intermediate

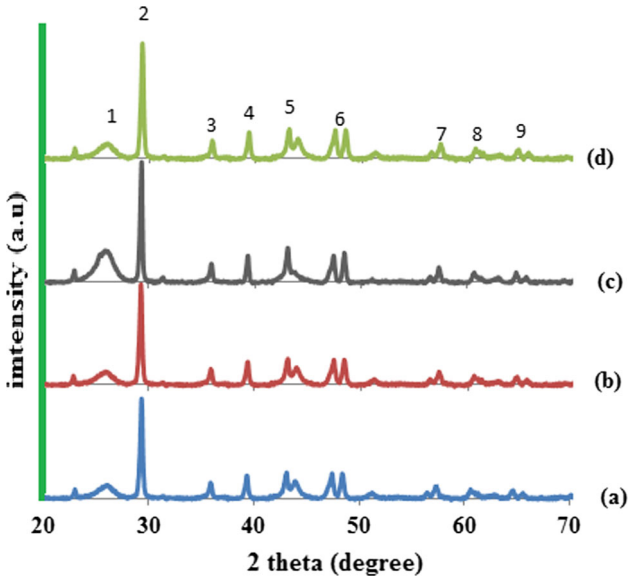

Fig. 10 XRD spectral of as-synthesized MWCNTs (*a*) 650 °C (*b*) 700 °C (*c*) 750 °C (*d*) 800 °C (*1* = graphitized MWCNTs; *2*, *3*, *6*, *8*, *9*=$CaCO_3$, CaO, Co_3O_4; *4*= Fe_2O_3/CoO, $Ca_2Fe_2O_5$; *5*= NiO/Co_3O_4; *7*= Fe_3O_4

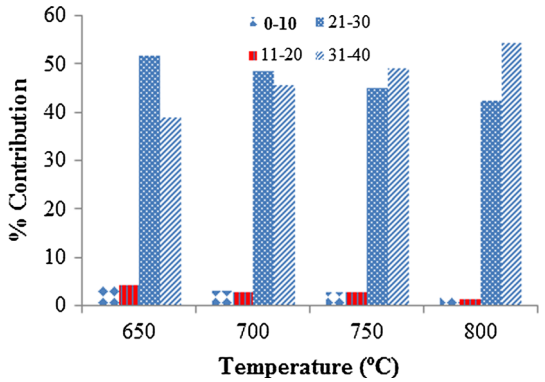

Fig. 11 Particle size distributions of the synthesized MWCNTs at 650, 700, 750 and 800 °C of 350 argon and 100 mL/min acetylene flow rate for 70 min reaction time

compound which are responsible for the catalyst deactivation or formation of amorphous carbon which perhaps covered the surface of carbon nanotubes [24]. This study showed that the MWCNTs yield is dependent on the deposition temperature and reaction time. The interaction between deposition temperature and growing time was more pronounced at 800 °C and 70 min, respectively. It can be concluded that deposition temperature and growing time at constant catalyst dosage have significant effect on the yield of carbon nanostructures. The MWCNTs prepared by CVD method from the tri-metallic catalyst supported on $CaCO_3$ was characterized to determine the quality of CNTs produced, and the results of various characterization are presented as follows.

3.9 XRD Pattern of MWCNTs

The XRD spectra of selected MWCNTs produced from Fe − Co − Ni/$CaCO_3$ catalyst at different temperatures (650, 700, 750 and 800 °C) are shown in Fig. 10.

According to Fig. 10, three major phases which represent carbon, calcium carbonate, and mixed oxides were noticed irrespective of the growing temperature. The diffraction peaks at $2\theta = 26.2°$ with a corresponding crystal planes (002) belongs to graphitized MWCNTs. According to Maccallini et al. [25], the presence of the crystal plane (002) signified multilayer coverage of the graphitized carbon on the supported catalytic metallic nanoparticles. In addition, the intensity of the peak observed at $2\theta = 26.2°$ increases with increasing temperature from 650 to 750 °C, which indicate that the extent of graphitization depends largely on the heating temperature. In addition, a clearly defined peak was noticed at $2\theta = 44.1°$ for MWCNTs produced at 750 °C compared to other heating temperatures. This further demonstrated that the MWCNTs produced at 750 °C may be highly crystalline devoid of defects as clearly shown in Fig. 10e. On the other hand, the intensity at $2\theta = 26.2°$ observed at 800 °C reduced, which signified weak peak. This showed that CNTs prepared at this temperature were tangled as evident in the HRSEM micrograph shown in Fig. 10f. Furthermore, the observed characteristics peaks around 29.8° and 36.1° were assigned to $CaCO_3$ and CaO and were peculiar to all the samples irrespective of heating temperature. The presence of CaO was attributed to the decomposition of $CaCO_3$ which occurred around at 610–810 °C as demonstrated in TGA profile shown in Fig. 1. Similar observation was reported by Schmitt et al. [18] who observed the presence of both CaO and $CaCO_3$ at 720 °C. While the residual $CaCO_3$, represents the unreacted $CaCO_3$ during the synthesis. The peak observed at $2\theta = 39.5°$ according to Bahgat et al. [9] was classified as mixed phase, which could either be Fe_2O_3 or CoO or $Ca_2Fe_2O_5$. This new mineral phase was formed based on the reaction between the support ($CaCO_3$) and the metallic oxides (Fe_2O_3 and CoO). Additionally, the new peak at $2\theta = 48.5°$ is assigned to $CaCO_3$, and similar intensity was observed irrespective of the temperature and thus not affected nor depend on the heating temperature. The peak corresponding to individual metallic particles (Fe, Co or Ni) was not detected possibly due to their low concentration, small particle size nature or easy dispersion onto the catalyst support. The peaks at $2\theta = 44°$ and approximately 46° with corresponding hkl planes (111) and (200) are characteristic peaks assigned to the NiO and Co_3O_4, respectively.

The particle size distribution of the synthesized CNTs was determined using the Scherrer equation presented in Fig. 11.

According to Fig. 11, it can be observed that the diameter of the produced CNTs increases with increasing production temperature and substantial number of the prepared carbon

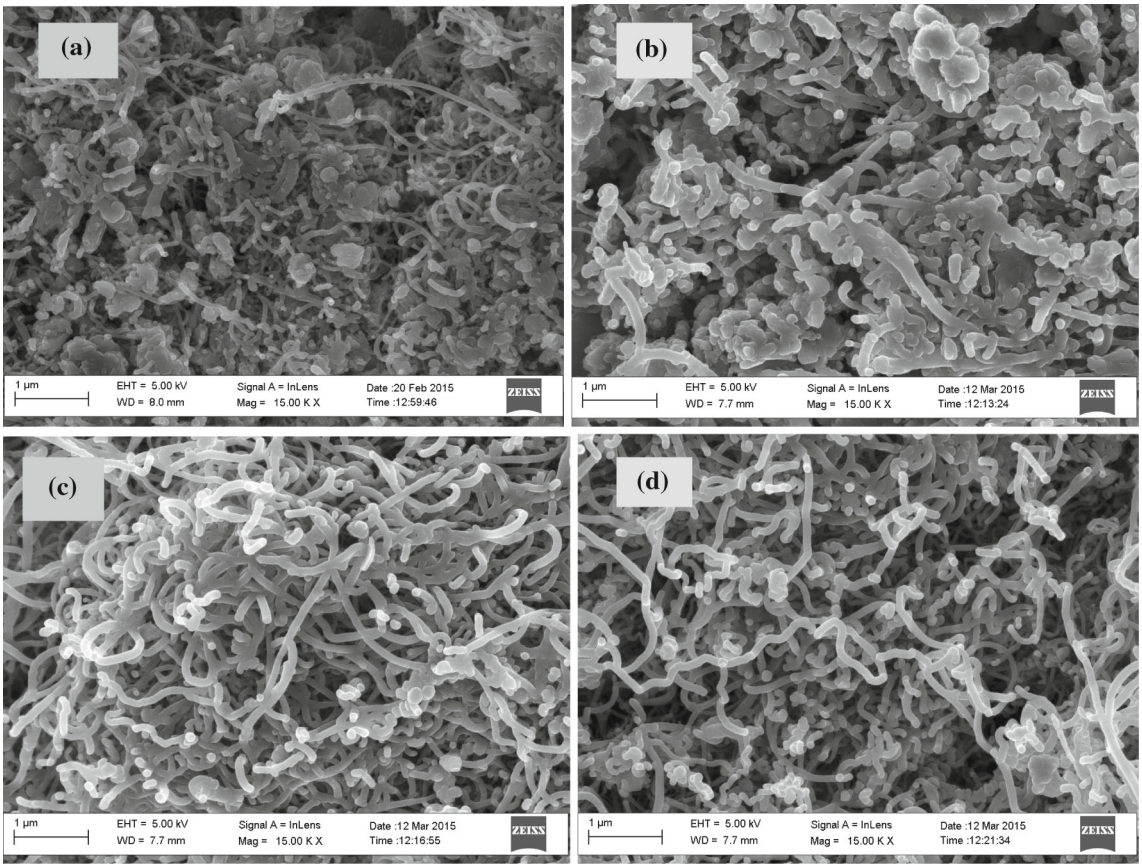

Fig. 12 The HRSEM micrographs of as-synthesized carbon nanotubes **a** 650 °C, **b** 700 °C, **c** 750 °C, **d** 800 °C at growing time of 70 min

nanostructure particles were in the range of 21–30 and 31–40 nm respectively. These results further demonstrated that increasing the growth temperature is directly proportional to the average diameter of CNTs and the particle sizes. This finding further supports the Charles law of kinetic theory of gases, which states that increase in the growth temperature correspond to increase in kinetic energy and diffusion rate of gas molecules in the growth chamber. This in turn increases the rate of decomposition of carbon precursor on $CaCO_3$ supported Fe–Ni–Co catalysts placed centrally in CVD reactor chamber. Thus, the average diameter and length of as-synthesised carbon nanotubes is increased as the growth temperature increased.

The surface morphology of the as-synthesized MWCNTs is presented in Fig. 12.

The HRSEM images show the effect of temperature on the morphology of MWCNTs. The effect of temperature was studied by varying the growing temperatures between 650 and 800 °C at constant time, argon flow rate and acetylene flow rate of 70 min, 350 and 100 mL/min respectively. It can be noticed that by increasing in the growth temperature from 650 to 800 °C, the growth density of CNTs on the surface of $CaCO_3$ supported Fe–Co–Ni catalyst also increased. According to Fig. 12a, the abundance of MWCNTs is relative small compare to metallic and residual support particles observed on the surface of CNTs. The presence of little stands of CNTs could be ascribed to incomplete nucleation process of CNTs at a temperature of 650 °C. Hence, the catalytic cracking of acetylene for the synthesis of carbon nanotubes was not favoured at the deposition temperature of 650 °C. In Fig. 12b, randomly distributed aggregated fibrous-like clusters of CNTs are produced at 700 °C. Notably, presence of an aggregation amorphous carbon, metallic, and support particles, and less ordered CNTs still persist.

However, at 750 and 800 °C, completely different carbonaceous nanostructures morphology was observed. A more densely populated MWCNTs structure consist of several strands of nearly uniform diameter containing negligible amount of residual $CaO/CaCO_3$ and metallic particles were observed. The presences of abundance CNTs with smooth outer wall distributed uniformly on the surface of supported catalyst may be due to the rapid decomposition of acetylene gas and $CaCO_3$ support at high heating temperature. Therefore, growth temperature of 750 and 800 °C favors the deposition of uniform diameter of MWCNTs in CVD equipment. The HRSEM and HRTEM micrographs (Figs. 12, 13)

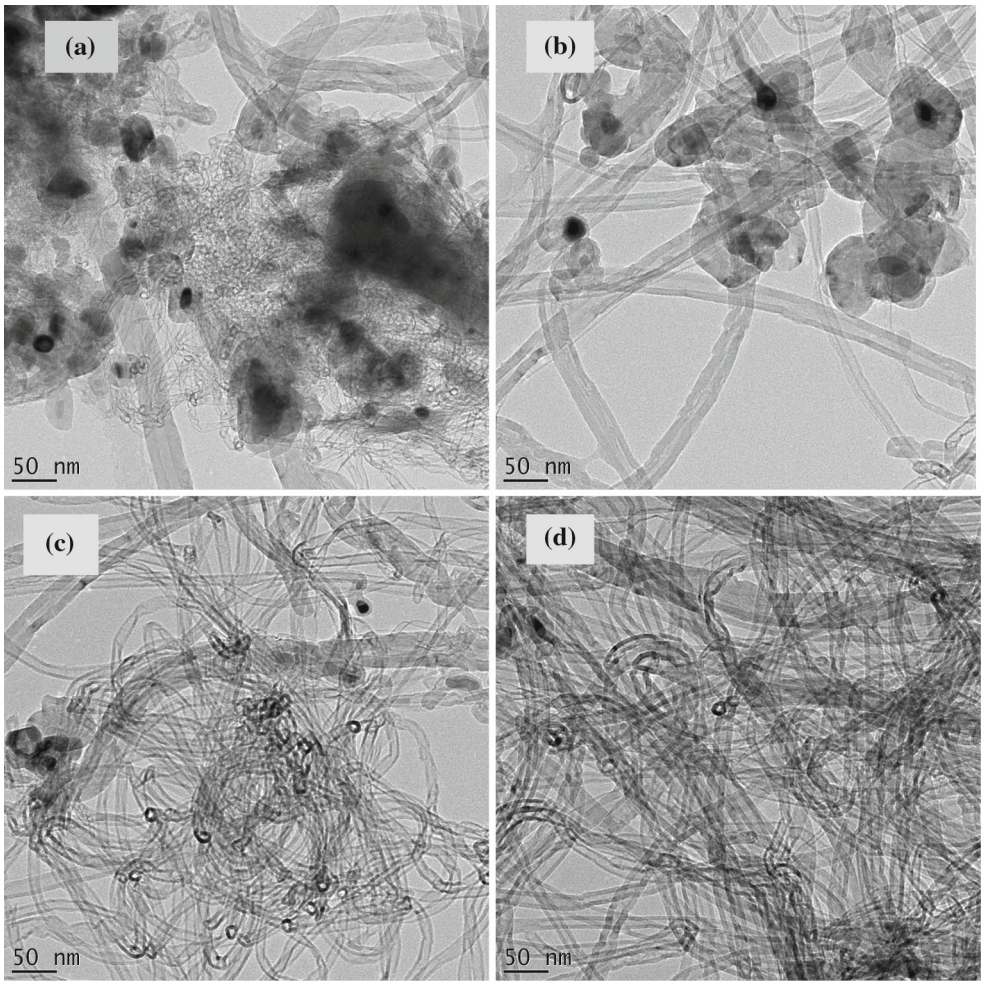

Fig. 13 The TEM micrographs showing the images of the as-synthesized carbon nanotubes **a** 650 °C, **b** 700 °C, **c** 750 °C, **d** 800 °C at growing time of 70 min

irrespective of the growing temperature revealed the presence of metallic and $CaCO_3$ support particles closely stick on to the walls of MWCNTs.

However, this degree of stickiness of metallic particles on the tubular structure was less pronounced at higher temperature and as such a clear defined tubular morphology of the carbon nanostructures was noticed as shown in Fig. 13c, d. This indicates that the CNTs formation followed a tip growth mechanism. A close examination of Fig. 12 revealed that as the deposition temperature increased, the amount of deposited CNTs and their corresponding diameter increases. This was confirmed in the physical appearance of the prepared CNTs at different temperature. Similar observations were reported by Mahmoodi and colleague, [26] during their investigation of the effect of temperature on the diameter of carbon nanotubes. It was found that as the growth temperature increases, the level of amorphous carbon, catalyst and support particles decreased and well-arranged arrays and highly crystalline CNTs were produced. The observed trend clearly complement the XRD results shown in Fig. 10 and however contradict the CNTs yield result shown in Fig. 8. Furthermore, the HRSEM results presented in Fig. 12a, b revealed poor-quality CNTs obtained at lower temperature. This mean that at lower temperature, carbon radical produced in the gas phase nucleate faster and quickly form the tube; however, the temperature is not enough to sustain the growth of the CNTs on the catalyst, thus caused the stunted development of the CNTs [26]. The HRSEM micrographs demonstrate that growth temperature influenced the quality of CNTs obtained. It was proved that at low temperature entangled CNTs with several structural defects were produced compared highly crystalline and untangled CNTs obtained at 800 °C.

Figures13a–d depicts the HRTEM images of MWCNTs produced at 650, 700, 750 and 800 °C respectively.

As shown in Fig. 13a, the HRTEM image revealed the formation of randomly aggregated filamentous strands of MWCNTs encapsulated with the large number of metal-

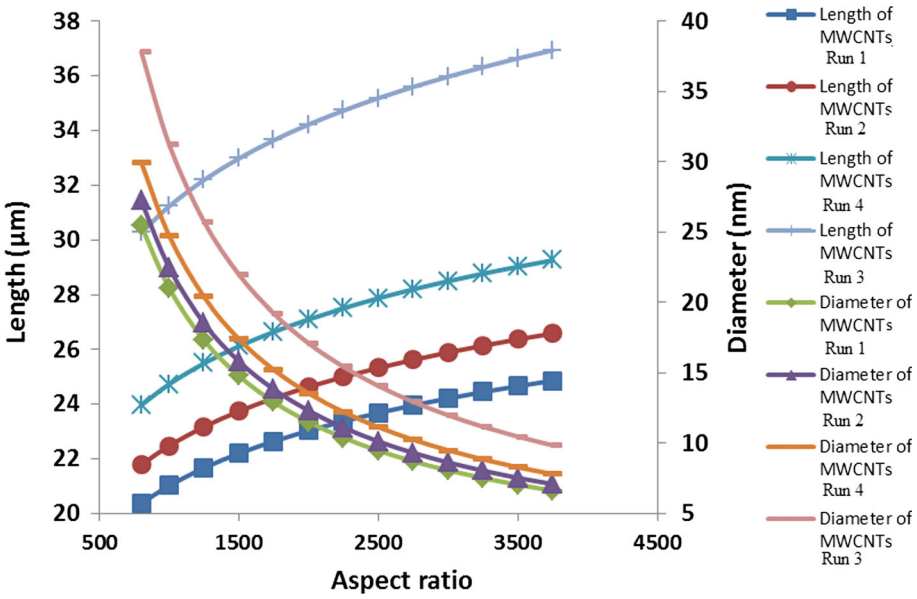

Fig. 14 Aspect ratio of various as-synthesized MWCNTs at (**a**) 650 °C (**b**) 700 °C (**c**) 750 °C (**d**) 800 °C

lic catalyst particles and the residual $CaO/CaCO_3$under the applied experimental conditions. According to Fig. 13b at 700 °C, it is obvious that the size (diameter) of the produced CNTs increases with increasing production temperature. In addition, a clearly defined strand of MWCNTs was obtained, which means that the temperature increment possibly influenced the microstructure of the prepared materials. It should be mentioned that catalyst and support materials particles are still embedded on surface, tip, and inner layer of the carbon nanostructures. Furthermore, a close observation of the MWCNTs produced at 750 and 800 °C revealed the presence of agglomerated, homogeneous and dense multi-walled carbon nanotubes encapsulated with lesser amount of metallic catalyst and support particles at the tips and inner walls of the tubes, respectively. The presence of little or no metallic particles on the CNT walls suggested strong interaction between the catalyst particle and the $CaCO_3$ support, which is an evidence of base growth mode. This strong interaction may be attributed to chemical affinity between the iron nanoparticle precursor and the $CaCO_3$ matrix. Generally, it was observed that the tubes are not completely straight but rather continuously hollow having different diameter and length. The walls are frequently bridged and some defects are also seen. This showed that the decomposition mechanism of acetylene gas decomposition on Fe–Co–Ni supported on $CaCO_3$ irrespective of the combustion temperature was the same.

Very importantly, there was no presence of bigger catalyst particles encapsulated by multi-walled carbon layers, as shown in Fig. 13d. The absence or no significant presence of amorphous carbon or catalyst metallic particles at 750 and 800 °C can be attributed to the non-porous nature of the support material $CaCO_3$, which possibly suppressed the amorphous carbon formation and accelerated CNTs growth.

On the other hand, the relationship between the length and the diameter (aspect ratio) obtained from the DLS analysis was established to significantly identify the best area of application of the synthesized MWCNTs. The aspect ratio is displayed in Fig.14.

The diameter of as-synthesized MWCNTs obtained from XRD was related to the D_h (hydrodynamic diameter) using modified Navier–Stokes equation shown in Eq. 5 [27].

$$D_h = \frac{L}{\ln(L/d) + 0.32} \tag{6}$$

where D_h is the hydrodynamic diameter, l is the length and d is the diameter of MWCNTs.

The average diameter (*Z*-average) also known as the hydrodynamic diameter (D_h) of the produced carbon nanotubes in the temperature ranges of 650–800 °C were determined using Dynamic Light Scattering (DLS). The hydrodynamic diameters of the MWCNTs were found to be 2908, 3110, 3422 and 4321 nm for samples obtained at 650, 700, 750 and 800 °C, respectively. The DLS result shows that the lengths of MWCNTs are directly proportional to the diameters and their respective production temperature. The result indicates that the actual diameter of the synthesized MWCNTs using the growth condition of 650, 700, 750 and 800 °C were 21.50, 22.48, 26.81 and 27.64 nm respectively, with corresponding aspect ratio of 878, 1000, 920, and 1164. Thus, the average diameter in the range of 21.5–27.64 nm reported in this study directly determined from the HRTEM micrographs falls within the acceptable range of a typical graphitized long-tube MWCNTs. The aspect ratio of all the synthesized MWCNTs shows that the MWCNTs are fitted in the area of composite and concrete reinforcement. This

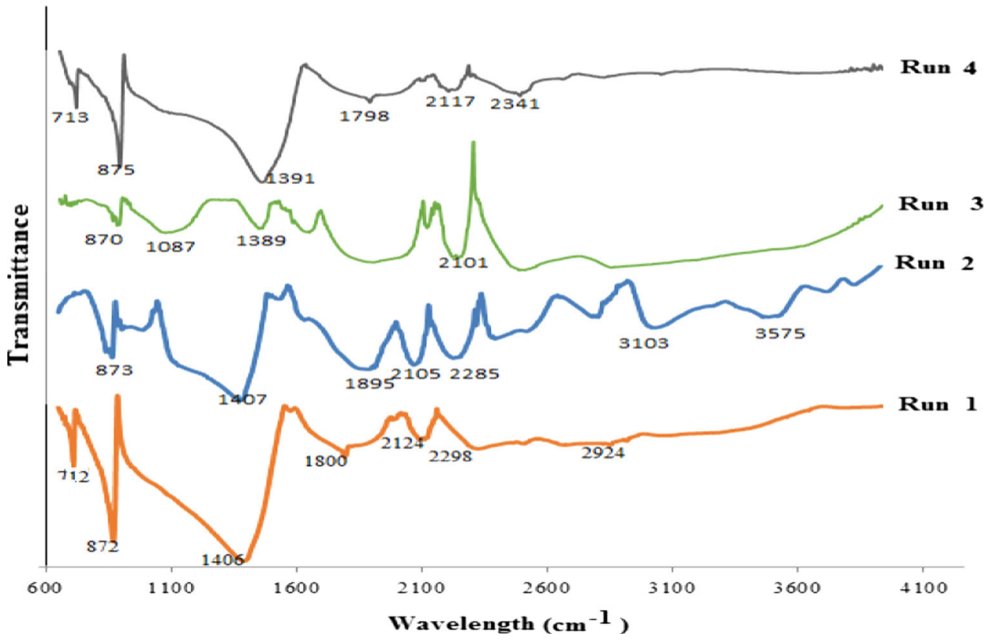

Fig. 15 The FTIR spectra of the as-synthesized carbon nanotubes (**a**) 650 °C (**b**) 700 °C, (**c**) 750 °C (**d**) 800 °C

property is in agreement with the report of Abu Al-Rub et al. [28].

The FTIR analysis was carried out to determine the surface functional groups present in the as-synthesized MWCNTs. Figure 15 shows the FTIR spectra of the as-synthesised MWCNTs.

The spectral presented in Fig. 15 shows the presence of C–C and C–O bending bond within the ranges of 600–1400 cm^{-1}, which is generally identified as the fingerprint region. These bonds are obvious in Run 1, 2, and 4 than run 3. The presence of surface water at 3103 cm^{-1} was only noticeable in MWCNTs produced at run 2, which was linked to the exposure of the MWCNTs to the surrounding environment after synthesis. The peaks around 1600 and 1800 cm^{-1} represent the presence of C=C double bond resulting from incomplete decomposition of acetylene during the catalytic cracking of the hydrocarbon material [28,29].

The surface area of the as-synthesized MWCNTs at the operating condition of 800 °C was determined using nitrogen adsorption BET. The determined surface area was found to be 262 m^2/g, which is higher than 40 m^2/g reported by Mhlanga and Coville, [27] for MWCNTs prepared from bimetallic catalyst Fe–Co/$CaCO_3$. The improvement in the surface area obtained in this study compared to what was reported Mhlanga and Coville, [27] may be due to the additional effect of Ni particles and acetylene flow rate used in this study. The pore volume and the pore size were also determined to be 0.091 cm^3/g and 3.231 nm respectively. The pore volume and the pore sizes give the area of the synthesized carbon nanotubes applications. The thermal analysis of the

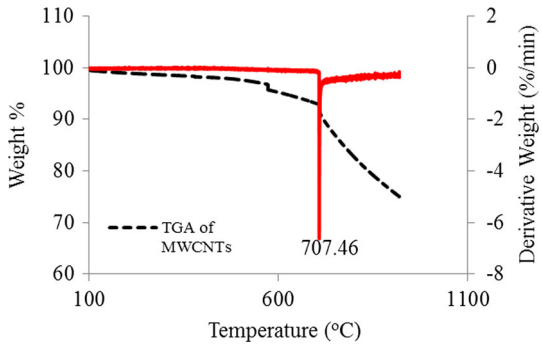

Fig. 16 TGA/DTA of MWCNTs at 800 °C

synthesis MWCNTs at the growth condition of 800 °C is as depicted in Fig.16.

The TGA/DTA shows the characteristic thermal behavior TGA/DTA of the synthesized MWCNTs. The TGA/DTA was used to determine the percentage purity, peak degradation temperature of the metallic catalyst and amorphous content of the MWCNTs. As shown in Fig. 16, it can be noticed that the prepared CNTs were thermally stable up to 570 °C, where carbon begins to oxidize and there was no any noticeable weight loss.

This suggests that the content of amorphous carbon in the sample is low. Beyond this temperature, a slight weight loss was observed and the remaining materials were linked to residual CaO and probably metallic catalyst particles (Fe–Co–Ni) [28,29]. Early studies have shown that absence or no substantial weight lost at a temperature above 450 °C of as-synthesised CNTs, signified crystalline and extent of

graphitization of the carbon species in the CNTs [10,29,30]. Similarly, the peak degradation temperature of the MWCNTs as determined from the DTA was 707.46 °C. This temperature shows the prepared CNTs are thermally stable and have high tendencies as possible application for reinforcement in composites mixture.

4 Conclusion

In summary, tri-metallic catalyst and multi-walled carbon nanotubes were successfully developed using wet impregnation and catalytic chemical vapor deposition methods. The effects of operating parameters such as mass of support, pre-calcination time, and pre-calcination temperature on the catalyst yield based on factorial experimental design was explored. The effect of growing time and deposition temperature on the morphologies and crystallinity of CNTs were also investigated. Based on the results obtained, the following conclusions were drawn: The highest catalyst yield of 92.04% was obtained at the optimal conditions of 8 g (mass of support), 110 °C (Pre-calcination temperature) and 8 h (pre-calcination time). The deposition temperature and growing time influenced the diameter of as-synthesized MWCNTs synthesized over the Fe–Co–Ni/$CaCO_3$. The diameter of MWCNTs was determined to be directly proportional to the growth temperature and the MWCNTs yield increases as the reaction time increases from 30 to 70 min. The results demonstrated that the ideal optimum deposition temperature and growing time to produce high-quantity and high-quality MWCNTs was about 800 °C and 70 min at constant argon and acetylene flow rate of 350 and 100 mL/min, respectively. The relationship between length and the diameter of the as-synthesized MWCNTs proves that the CNTs developed are a long-tube MWCNTs with aspect ratio ranges from 800 to 1200. The study shows that Fe–Co–Ni/$CaCO_3$ catalyst developed using wet impregnation method proves effective and efficient in the growth of long-tube MWCNTs in a CVD reactor.

Acknowledgements Financial support received from Tertiary Education Tax Fund (TETFUND) Nigeria with Grant Number TETFUND/FUTMINNA/NRF/2014/01 is greatly appreciated. The authors are grateful to Centre for Genetic Engineering and Biotechnology, Federal University of Technology, Minna, for the assistance rendered during sample analysis. The authors wish to appreciate the following people that helped in analyzing the samples: Dr. Remy Bucher (XRD, ithemba Labs), Dr. Franscious Cummings (HRTEM, Physics department, University of the Western Cape (UWC), South Africa), Andrian Joseph (HRSEM, Physics department, UWC, South Africa).

Compliance with Ethical Standards

Conflict of interest The authors declared no conflicts of interest.

References

1. Allaedini, G.; Tasirin, S.M.; Aminayi, P.; Yaakob, Z.; Talib, M.Z.M.: Bulk production of bamboo-shaped multi-walled carbon nanotubes via catalytic decomposition of methane over tri-metallic Ni–Co–Fe catalyst. React. Kinet. Mech. Catal. **116**, 385–396 (2015)
2. Amiri, A.; Maghrebi, M.; Baniadam, M.; Zeinali, H.S.: One-pot, efficient functionalization of multi-walled carbon nanotubes with diamines by microwave method. Appl. Surf. Sci. **257**, 10261–10266 (2011)
3. Iijima, S.: Helical microtubules of graphitic carbon. Nature **354**, 56–58 (1991)
4. Jeong, S.W.; Son, S.Y.; Lee, D.H.: Synthesis of multi-walled carbon nanotubes using Co–Fe–Mo/Al_2O_3 catalytic powders in a fluidized bed reactor. Adv. Powder Technol. **21**, 93–99 (2010)
5. Voelskow, K.; Becker, M.J.; Xia, W.; Muhler, M.; Turek, T.: The influence of kinetics, mass transfer and catalyst deactivation on the growth rate of multiwalled carbon nanotubes from ethene on a cobalt-based catalyst. Chem. Eng. J. **244**, 68–74 (2014)
6. Yang, X.; Zou, T.; Shi, C.; Liu, E.; He, C.; Zhao, N.: Effect of carbon nanotube (CNT) content on the properties of in-situ synthesis CNT reinforced Al composites. Mater. Sci. Eng. **A660**, 11–18 (2016)
7. Kavecký, S.; Valúchova, J.; Čaplovičová, M.; Heissler, S.; Šajgalík, P.; Janek, M.: Nontronites as catalyst for synthesis of carbon nanotubes by catalytic chemical vapor deposition. Appl. Clay Sci. **114**, 170–178 (2015)
8. Liu, W.W.; Chai, S.P.; Mohamed, A.R.; Hashim, U.: Synthesis and characterization of graphene and carbon nanotubes: a review on the past and recent developments. J. Ind. Eng. Chem. **20**, 1171–1185 (2014)
9. Bahgat, M.; Farghali, A.A.; El Rouby, W.M.A.; Khedr, M.H.: Synthesis and modification of multi-walled carbon nanotubes (MWCNTs) for water treatment applications. J. Anal. Appl. Pyrol. **92**, 307–313 (2011)
10. Chiwaye, N.; Jewell, L.L.; Billing, D.G.; Naidoo, D.; Ncube, M.; Coville, N.J.: In situ powder XRD and Mössbauer study of Fe–Co supported on $CaCO_3$. Mater. Res. Bull. **56**, 98–106 (2014)
11. Motchelaho, M.A.M.; Xiong, H.; Moyo, M.; Jewell, L.L.; Coville, N.J.: Effect of acid treatment on the surface of multiwalled carbon nanotubes prepared from Fe–Co supported on $CaCO_3$: correlation with Fischer–Tropsch catalyst activity. J. Mol. Catal. A Chem. **335**, 189–198 (2011)
12. Duan, X.; Wang, D.; Qian, G.; Walmsley, J.C.; Holmen, A.; Chen, D.; Zhou, X.: Fabrication of K-promoted iron/carbon nanotubes composite catalysts for the Fischer–Tropsch synthesis of lower olefins. J. Energy Chem. **0**, 1–7 (2016)
13. Cheng, J.; Zhang, X.; Luo, Z.; Liu, F.; Ye, Y.; Yin, W.; Liu, W.; Han, Y.: Carbon nanotube synthesis and parametric study using $CaCO_3$ nanocrystals as catalyst support by CVD. Mater. Chem. Phys. **95**, 5–11 (2006)
14. Chen, C.M.; Dai, Y.M.; Huang, J.W.; Jehng, J.M.: Intermetallic catalyst for carbon nanotubes (CNTs) growth by thermal chemical vapor deposition method. Carbon **44**, 1808–1820 (2006)
15. Yeoh, W.M.; Lee, K.Y.; Chai, S.P.; Lee, K.T.; Mohamed, A.: Synthesis of high purity multi-walled carbon nanotubes over Co–Mo/MgO catalyst by the catalytic chemical vapour deposition of methane'. New Carbon Mater. **24**, 60041–60044 (2009)
16. Taleshi, F.: Evaluation of New Processes to Achieve a High Yield of Carbon Nanotubes by CVD Method. Int. Nano Lett. **2**, 23–28 (2012)
17. Mhlanga, S.D.; Mondal, K.C.; Carter, R.; Witcomb, M.J.; Coville, N.J.: The effect of synthesis parameters on the catalytic synthesis of multiwalled carbon nanotubes using Fe–Co/$CaCO_3$ catalysts. S. Afr. J. Chem. **62**, 67–76 (2009)

18. Schmitt, T.C.; Biris, A.S.; Miller, D.W.; Biris, A.R.; Lupu, D.; Trigwell, S.; Rahman, Z.U.: Analysis of effluent gases during the CCVD growth of multi-wall carbon nanotubes from acetylene. Carbon **44**, 2032–2038 (2006)
19. Magrez, A.; Seo, J.W.; Smajda, R.; Mioni, M.; Forró, L.: Catalytic CVD synthesis of carbon nanotubes: towards high yield and low temperature growth. Materials **3**, 4871–4891 (2010)
20. Li, Z.; Dervishi, E.; Xu, Y.; Ma, X.; Saini, V.; Biris, A.S.; Little, R.; Lupu, D.: Effects of the Fe–Co interaction on the growth of multiwall carbon nanotubes. J. Chem. Phys. **129**, 074712–074717 (2008)
21. Khavarian, M.; Chais, S.P.; Tan, S.H.; Mohamed, A.R.: Effect of different parameters on the morphology of carbon nanotubes structure grown by floating catalyst method. J. Appl. Sci. **11**, 2382–2387 (2011)
22. Kariim, I.; Abdulkareem, AS.; Abubakre, OK.; Mohammed, IA.; Bankole, MT.; Tijani, JO.: Studies on the suitability of alumina as bimetallic catalyst support for MWCNTs growth in a CVD reactor. First International Engineering Conference, School of Engineering and Engineering Technology, Federal University of Technology, Minna, Nigeria, pp. 296–305 (2015)
23. Allaedini, G.; Aminayi, P.; Tasirin, S.M.: Methane decomposition for carbon nanotube production: optimization of the reaction parameters using response surface methodology. Chem. Eng. Res. Des. **112**, 163–174 (2016). (2016)
24. Hanaei, H.: The interaction effects of synthesis reaction temperature and deposition time on carbon nanotubes (CNTs) yield. Int. J. Mater. Sci. **1**, 54–61 (2013)
25. Maccallini, E.; Tsoufis, T.; Policicchio, A.; La Rosa, S.; Caruso, T.; Chiarello, G.; Colavita, E.; Formoso, V.; Gournis, D.; Agostino, R.G.: A spectro-microscopic investigation of Fe–Co bimetallic catalysts supported on MgO for the production of thin carbon nanotubes. Carbon **48**, 3434–3445 (2010)
26. Mahmoodi, A.; Ghoranneviss, M.M.; Mojtahedzadeh, S.H.; Haji, H.; Eshghabadi, M.: Various temperature effects on the growth of carbon nanotubes (CNTs) by thermal chemical vapor deposition (TCVD) method. Int. J. Phys. Sci. **7**(6), 949–952 (2012)
27. Mhlanga, S.D.; Coville, N.J.: Iron–cobalt catalysts synthesized by a reverse micelle impregnation method for controlled growth of carbon nanotubes. Diam. Relat. Mater. **17**, 1489–1493 (2008)
28. Nair, N.; Kim, W.J.; Braatz, R.D.; Strano, R.D.: Dynamics of suspended single-walled carbon nanotubes in a centrifugal field. Langmuir **24**, 1790–1795 (2008)
29. Al-Rub, R.K.A.; Ashour, A.I.; Tyson, B.M.: On the aspect ratio effect of multi-walled carbon nanotube reinforcements on the mechanical properties of cementitious nanocomposites. Constr. Build. Mater. **35**, 647–655 (2012)
30. Afolabi, A.S.; Abdulkareem, A.S.; Mhlanga, S.D.; Iyuke, S.E.: Synthesis and purification of bimetallic catalysed carbon nanotubes in a horizontal CVD reactor. J. Exp. Nanosci. **6**(3), 248–262 (2011)